Comparative study of the photo-protective and anti-melanogenic properties of gomisin D, J and O

JOONG SUK JEON[1], HE MI KANG[1], SUN YOUNG PARK[2] and YOUNG-WHAN CHOI[1]

[1]Department of Horticultural Bioscience, Pusan National University, Miryang, Gyeongsangnam-do 50463; [2]Bio-IT Fusion Technology Research Institute, Pusan National University, Busan 46241, Republic of Korea

Received July 24, 2021; Accepted October 20, 2021

DOI: 10.3892/mmr.2021.12524

Abstract. Skin cancer is the most common human malignancy worldwide and solar ultraviolet (UV) radiation is known to serve an important role in its pathogenesis. Natural candidate compounds with antioxidant, photoprotective and anti-melanogenic effects were investigated against the background of skin photoprotective and anti-melanogenic properties. Gomisin D, J and O are dibenzocyclooctadiene lignans present in *Kadsura* medicinal plants and possess several pharmacological activities. In this study, the functions and mechanisms underlying the effects of gomisin D, J and O in UVA-and UVB-irradiated keratinocytes and α-melanocyte stimulating hormone (α-MSH)-stimulated melanocytes were explored. Following UVA and UVB irradiation, keratinocytes were treated with gomisin D, J and O, and keratinocyte viability, lactate dehydrogenase (LDH) release, intracellular reactive oxygen species (ROS) production and apoptosis were examined. The results demonstrated that gomisin D and J improved keratinocyte viability and reduced LDH release under UVA and UVB irradiation. Intracellular ROS production induced by UVA and UVB irradiation was suppressed by gomisin D and J. In addition, Annexin V and TUNEL staining analysis indicated that gomisin D and J have significant anti-apoptotic effects on UVA-and UVB-irradiated keratinocytes. After α-MSH stimulation, melanocytes were treated with gomisin D, J and O, and the changes in melanocyte viability, intracellular melanin content, intracellular tyrosinase activity, and mechanisms underlying these changes were examined. Gomisin D markedly inhibited the α-MSH-induced increase in intracellular melanin content and tyrosinase activity. Mechanistically, gomisin D reduced the protein and mRNA expression levels of microphthalmia-associated transcription factor (MITF), tyrosinase, tyrosinase-related protein (TRP)-1 and TRP-2 in α-MSH-stimulated melanocytes. In addition, gomisin D markedly downregulated α-MSH-induced phosphorylation of protein kinase A and cAMP response element binding protein, which are known to be present upstream of the MITF, tyrosinase, TRP-1 and TRP-2 genes. Overall, gomisin D has photoprotective and anti-melanogenic effects; these findings provide a basis for the production of potential brightening and photoprotective agents using natural compounds such as gomisin D.

Correspondence to: Professor Young-Whan Choi, Department of Horticultural Bioscience, Pusan National University, 1268-50 Samnangjin-ro, Miryang, Gyeongsangnam-do 50463, Republic of Korea
E-mail: ywchoi@pusan.ac.kr

Professor Sun Young Park, Bio-IT Fusion Technology Research Institute, Pusan National University, 2 Busandaehak-ro 63 beon-gil, Busan 46241, Republic of Korea
E-mail: sundeng99@pusan.ac.kr

Abbreviations: UV, ultraviolet; LDH, lactate dehydrogenase; α-MSH, α-melanocyte stimulating hormone; cAMP, cyclic AMP; CREB, cAMP response element binding protein; MITF, microphthalmia-associated transcription factor; PKA, protein kinase A; ROS, reactive oxygen species; TRP-1, tyrosinase-related protein-1; TRP-2, tyrosinase-related protein-2

Key words: Gomisin D, J and O, photo-protection, keratinocyte, anti-melanogenesis, melanocyte

Introduction

Kadsura medicinal plants are Traditional Chinese herbs with a variety of biological properties, including antimicrobial, anti-human immunodeficiency virus (HIV), anti-fungal, anti-lipid peroxidation, anti-hepatitis, anti-inflammatory and antitumor properties (1,2). Modern pharmacological studies have shown that most pharmacological and biological actions of *Kadsura* medicinal plants can be attributed to dibenzocyclooctadiene lignans, which consist of >100 related compounds. Gomisin D, J and O are dibenzocyclooctadiene lignans extracted from the widely used medicinal plant *Kadsura*, which is well known for its safety and pharmacological effects, such as antioxidant, anti-inflammatory, antitumor, neuroprotective and anti-hyperglycemic activities (3,4). Given the pharmacological properties of dibenzocyclooctadiene lignans, the efficacy of gomisin D, J and O in photo-protection and anti-melanogenesis is worth exploring.

Solar ultraviolet (UV) radiation, characterized as UVA (320-400 nm), UVB (280-320 nm) and UVC (100-280 nm), are the most important environmental factors that cause skin cancer and photoaging due to cytotoxicity, genotoxicity and phototoxicity (5). In particular, UVA and UVB radiation

constitute 95% and >3% of the daily UV irradiation (6). UVA irradiation can induce reactive oxygen species (ROS) production either indirectly or directly; these ROS penetrate the epidermis and/or the epidermal layer of the skin, resulting in oxidative damage and cell death (7). UVB irradiation is predominantly absorbed by chromophores, such as nuclear DNA, which initiate this series of processes (8,9). Over the past few decades, UV radiation has become a serious public health problem and continues to be a worldwide risk factor (10-12). UV irradiation causes direct and consistent stimulation of keratinocytes, which accounts for ~95% of the skin epidermal cell mass (13). Keratinocytes act as the first barrier to primary microbial, chemical and physical hazards, and defend against UVA and UVB radiation. When keratinocytes are exposed to UVA and UVB, intracellular ROS are generated and trigger apoptosis (14-16).

Melanocytes within melanosomes regulate the production and amount of melanin pigment, which plays a key role in the biological defense of the skin epidermis, and their dysregulation leads to hyperpigmentation and dyspigmentation (17,18). Melanocytes are distributed in the stratum basales of the epidermis of the skin and are affected by sunlight exposure, ROS, cyclic AMP (cAMP) level-elevating agents and α-melanocyte stimulating hormone (α-MSH) (19,20). Tyrosinase is an evolutionarily conserved copper-containing metalloprotein that plays an important role in melanogenesis. Tyrosinase, a member of the type-3 copper protein family, plays an important role in monophenol monooxygenase, catecholase and diphenolase. Downregulation of tyrosinase, tyrosinase-related protein-1 (TRP-1) and tyrosinase-related protein-2 (TRP-2) have distinct catalytic functions. TRP-1 is a 5,6-dihydroxyindole-2-carboxylic acid oxidase and TRP-2 is a dopachrome tautomerase (21,22). Additionally, microphthalmia-associated transcription factor (MITF) is a transcription factor that regulates the transcription of numerous downstream genes, such as tyrosinase, TRP-1 and TRP-2 (23). Phosphorylation of cAMP-dependent protein kinase A (PKA) and cAMP response element-binding protein (CREB) is known to play critical roles in MITF transcription and translation (24). In the present study, dibenzocyclooctadiene lignans (gomisin D, J and O) were comprehensively investigated and their photo-protective and anti-melanin properties were evaluated.

Materials and methods

Reagents and chemicals. Gomisin D (cat. no. 60546-10-3; purity, >98%), gomisin J (cat. no. 66280-25-9; purity, >98%) and gomisin O (cat. no. 72960-22-6; purity, >98%) were purchased from Wuhan ChemFaces Biochemical Co., Ltd. Chemical structure and properties are presented in Fig. 1A and Table I, respectively.

Dulbecco's modified Eagle's medium (DMEM), fetal bovine serum (FBS), phosphate-buffered saline (PBS), penicillin and streptomycin were obtained from Gibco (Thermo Fisher Scientific, Inc.). The Cell Counting Kit-8 (CCK-8) assay kit, dimethyl sulfoxide (DMSO), 3,4-dihydroxyphenylalanine (L-DOPA), α-MSH, Signal Boost Immunoreaction Enhancer kit assay, bovine serum albumin (BSA) and 4',6-diamidino-2-phenylindole (DAPI) were obtained from Sigma-Aldrich (Merck KGaA). A cytotoxicity detection kit was purchased from Roche Diagnostics. The following were obtained from Thermo Fisher Scientific, Inc.: 5-(and-6)-chloromethyl-2',7'-dichlorodihydrofluorescein diacetate acetyl ester (CM-H2DCFDA), APO-BrdU™ transferase dUTP nick end labeling (TUNEL) assay kit, high-capacity cDNA reverse transcription kit, SYBR Green qPCR master mix, Mammalian Protein Extraction Reagent (M-PER) and Pierce ECL western blotting substrate. The fluorescein isothiocyanate (FITC) Annexin V/Dead Cell Apoptosis Kit was purchased from Invitrogen (Thermo Fisher Scientific, Inc.). The RNeasy Mini Kit was purchased from Qiagen GmbH. The Bio-Rad protein assay kit and Mini-PROTEAN Precast Gels were obtained from Bio-Rad Laboratories, Inc. Hybond polyvinylidene difluoride membranes were obtained from Amersham (Cytiva). Antibodies against tyrosinase (cat. no. sc-15341), TRP-1 (cat. no. sc-25543), TRP-2 (cat. no. sc-25544) were obtained from Santa Cruz Biotechnology (USA). MITF (cat. no. 12590), phosphorylated (p)-PKA (cat. no. 4781), PKA (cat. no. 4782), p-CREB (cat. no. 9198), CREB (cat. no. 9197), α-tubulin (cat. no. 2144) and HRP-conjugated anti-rabbit IgG (cat. no. 7074) antibodies were obtained from Cell Signaling Technology, Inc. Alexa Fluor 488-conjugated anti-rabbit antibody (1:500; cat. no. A-21206) was obtained from Thermo Fisher Scientific, Inc.

Cell culture. Keratinocytes (HaCaT; cat. no. 300493; CLS Cell Lines Service GmbH) and melanocytes (B16F10; cat. no. CRL-6475 American Type Culture Collection) were cultured in DMEM supplemented with 10% (v/v) FBS and 1% (v/v) penicillin and streptomycin solution and cultured at 37˚C with 5% CO_2. The experiments were performed using cells in the logarithmic growth phase. Cell growth was observed regularly and the medium was changed every 2-3 days. Cells treated with DMSO (1%) alone were used as controls in all the experiments.

UVA and UVB irradiation. For UVA and UVB exposure, keratinocytes were exposed to UVA (20 J/cm^2) and UVB (50 mJ/cm^2) irradiation (Bio-Link BLX-365; Vilber Lourmat Deutschland GmbH) with 5x8 W tubes that emit most of their energy with an emission peak at 365 nm (UVA) and 312 nm (UVB) (23,24).

Cell viability and cytotoxicity measurement through the CCK-8 and lactate dehydrogenase (LDH) analysis. The viability of keratinocytes irradiated with UVA (20 J/cm^2) and UVB (50 mJ/cm^2) after pretreatment with 10, 20, 30, 40 and 80 μM gomisin D, J and O at 37˚C for 1 h was quantified. For cell viability analysis, the CCK-8 assay kit reagents were added to HaCaT keratinocytes (~2x10^4 cells per well) and B16F10 melanoma cells (~2x10^4 cells per well) according to the manufacturer's instructions and incubated at 37˚C for 4 h. A cytotoxicity detection kit was used to determine extracellular LDH release in HaCaT keratinocyte culture medium. Absorbance was analyzed at 450 nm (CCK-8) and 490 nm (LDH) using a VICTOR Multilabel Plate Reader (PerkinElmer, Inc.).

Intracellular ROS production evaluation in keratinocytes. Intracellular ROS levels were analyzed using CM-H2DCFDA. All procedures were performed according to the manufacturer's instructions. In brief, after the addition of gomisin D, J and O (30 μM) the cells were incubated at 37˚C for 1 h.

Table I. Chemical and physical properties of gomisin D, J and O.

Properties	Gomisin D	Gomisin J	Gomisin O
Molecular weight (g/mol)	530.6	388.5	416.5
Molecular formula	$C_{28}H_{34}O_{10}$	$C_{22}H_{28}O_6$	$C_{23}H_{28}O_7$
XLogP3-AA	3.5	4.6	4
Hydrogen bond donor count	2	2	1
Hydrogen bond acceptor count	10	6	7
Rotatable bond count	3	4	4
Exact mass (g/mol)	530.21519728	388.18858861	416.18350323
Monoisotopic mass (g/mol)	530.21519728	388.18858861	416.18350323
Topological polar surface area (Å^2)	122.0	77.4	75.6
Heavy atom count	38	28	30
Formal charge	0	0	0
Complexity	871	457	574
Isotope atom count	0	0	0
Defined atom stereocenter count	0	2	3
Undefined atom stereocenter count	5	0	0
Defined bond stereocenter count	0	0	0
Undefined bond stereocenter count	0	0	0
Covalently-bonded unit count	1	1	1
Canonicalized compound	Yes	Yes	Yes

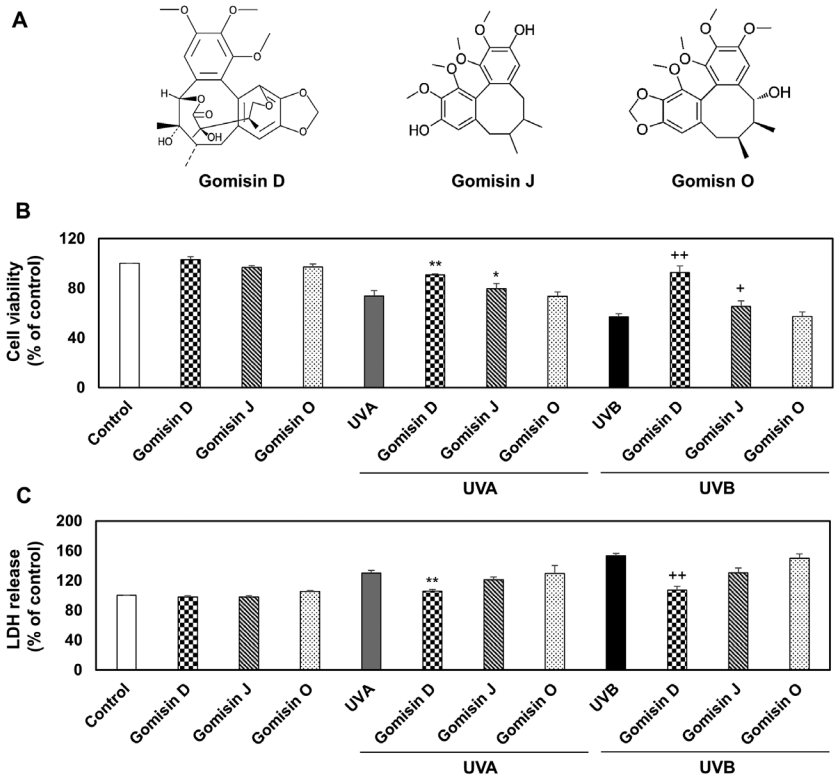

Figure 1. Keratinocyte viability and cytotoxic effects of gomisin D, J and O under UVA, UVB or non-irradiation conditions. (A) Structures of gomisin D, J and O. HaCaT keratinocytes were pretreated with gomisin D, J and O (30 μM) for 1 h. The keratinocytes were then irradiated with UVA (20 J/cm^2) and UVB (50 mJ/cm^2) for 24 h. (B) The percentage of viable keratinocytes was assessed using a Cell Counting Kit-8 assay. (C) The percentage of cytotoxicity was measured using an LDH assay. *P<0.05 and **P<0.01 vs. UVA-irradiated group; $^+$P<0.05 and $^{++}$P<0.01 vs. UVB-irradiated group. Data are expressed as the mean ± SD (n=3). UV, ultraviolet; LDH, lactate dehydrogenase.

Cells were subsequently exposed to UVA (20 J/cm^2) and UVB (50 mJ/cm^2) at 37˚C for 24 h. The HaCaT keratinocytes (~5x10^4 cells per well) were washed with PBS and incubated with CM-H2DCFDA at 25˚C for 0.5 h in the dark. Thereafter,

the generation of intracellular ROS was visualized using a Carl Zeiss fluorescence microscope (Carl Zeiss AG) and measured based on a fluorescence unit using a fluorescent dye in a flow cytometer (Fit NxT Flow Cytometer; Thermo Fisher Scientific, Inc.). Data were analyzed using Attune NxT Flow Cytometer software version 3.1.2 (Invitrogen; Thermo Fisher Scientific, Inc.).

Apoptosis analysis. After treatment, HaCaT keratinocytes (~5x10^4 cells per well) were trypsinized and centrifuged at 200 x g at 25˚C for 3 min. Subsequently, the obtained cells were treated according to the instructions of the FITC Annexin V/Dead Cell Apoptosis Kit and TUNEL assay kit. Briefly, keratinocytes were rinsed twice with PBS, and keratinocytes in Annexin binding buffer were obtained and mixed with FITC/Annexin V (component A) and propidium iodide (PI) working solution. After incubation at room temperature for 15 min in the dark, keratinocyte apoptosis was measured using a flow cytometer (Fit NxT Flow Cytometer). The percentages of early and late apoptotic cells were calculated using Attune NxT Flow Cytometer software version 3.1.2 (Invitrogen; Thermo Fisher Scientific, Inc.). The keratinocytes in the different groups were treated with 4% paraformaldehyde solution at 25˚C for 1 h and then the TUNEL assay kit was used to determine apoptosis according to the manufacturer's instructions. The nuclei were stained using DAPI mounting media (Sigma-Aldrich; Merck KGaA) for 0.5 min at room temperature. Using a Carl Zeiss fluorescence microscope (Carl Zeiss AG) three fields were observed. The percentage of TUNEL-positive cells was calculated using Attune NxT Flow Cytometer software (Invitrogen; Thermo Fisher Scientific). Apoptotic cells (TUNEL-positive cells) were determined using a Carl Zeiss fluorescence microscope (Carl Zeiss AG) and flow cytometry (Fit NxT Flow Cytometer).

Analysis of intracellular melanin content and tyrosinase activity. Intracellular melanin content and tyrosinase activity assays were performed using a slight modification of a previously reported procedure (25). Melanocytes (~4x10^4 cells per well) were treated with α-MSH (0.5 μM) in wells containing gomisin D, J and O (30 μM) at 37˚C for 48 h. Then, the melanocytes were washed with ice-cold PBS, trypsinized using trypsin-EDTA and centrifuged at 500 x g at 25˚C for 5 min. The melanocyte pellet was dissolved in a buffer containing 1N NaOH in 10% DMSO, lysed at 80˚C for 1 h and then centrifuged at 20,000 x g at 25˚C for 5 min. The relative melanin content was determined by measuring the absorbance at 475 nm using a VICTOR Multilabel Plate Reader. Intracellular tyrosinase activity was determined by measuring the rate of dopachrome production using L-DOPA. Melanocytes were washed with ice-cold PBS and lysed in PBS containing 1% (w/v) Triton X-100. The tyrosinase substrate L-DOPA (2 mg/ml) was prepared in phosphate lysis buffer. Each extract was placed in a well of a 96-well plate, and enzyme analysis was initiated by adding L-DOPA solution. Absorbance was measured at 475 nm using a VICTOR Multilabel Plate Reader and read every 10 min for 1 h in the dark. The end-point value of each measurement was expressed as a percentage of the control. Arbutin (A, 0.5 mg/ml) was used as a positive control.

Reverse transcription-quantitative (RT-q)PCR. Total RNA was isolated from each group of melanocytes using the RNeasy Mini Kit. RT was performed using the high-capacity cDNA reverse transcription kit according to the manufacturer's instructions to obtain the first strand of cDNA. The strand was then used as a template for qPCR using a Bio-Rad Chromo4™ instrument (Bio-Rad Laboratories, Inc.) and SYBR Green qPCR master mix. PCR was performed under pre-denaturation at 95˚C for 5 min, denaturation at 95˚C for 15 sec and annealing at 55-58˚C for 30 sec. GAPDH was used as an internal reference for tyrosinase, TRP-1 and TRP-2. The relative expression levels of the target genes were calculated using the $2^{-\Delta\Delta Cq}$ method (26). Primer sequences were as follows: tyrosinase sense, 5'-ggccagctttcaggcagaggt-3' and anti-sense, 5'-tggtgcttcatgggcaaaatc-3'; TRP-1 sense, 5'-agccccaactctgtcttttc-3' anti-sense, 5'-ggtctccctacatttccagc-3'; TRP-2 sense, 5'-tccagaagtttgacagccc-3' and anti-sense, 5'-ggaaggagtgagccaagttatg-3'; and GAPDH sense, 5'-aggtggtctcctctgacttc-3' and anti-sense, 5'-taccaggaaatgagcttgac-3'.

Western blotting. Melanocytes (~4x10^4 cells/well) were harvested and lysed using M-PER. All procedures were performed according to the instructions set by the manufacturer. All protein concentrations were determined using a Bio-Rad protein assay kit, according to the manufacturer's instructions. The loading buffer was then added to the protein supernatant and the solution was mixed. The mixture was boiled at 80˚C for 10 min, and proteins (30 μg protein/lane) were separated via 7.5% Mini-PROTEAN Precast Gels and transferred onto a Hybond polyvinylidene difluoride membrane using a Trans-Blot SD semi-dry transfer cell. Immunodetection was performed using antibodies against tyrosinase (1:1,000), TRP-1 (1:1,000), TRP-2 (1:1,000) MITF (1:1,000), p-PKA (1:1,000), PKA (1:1,000), p-CREB (p 1:1,000), CREB (1:1,000) and α-tubulin (1:1,000) and the Signal Boost Immunoreaction Enhancer kit assay. The membrane was incubated overnight with the primary antibodies at 4˚C. The secondary antibody (HRP-conjugated anti-rabbit IgG; 1:5,000) was added to the membrane and incubated at room temperature for 1 h. The protein bands were observed using an enhanced Pierce ECL western blotting substrate and semi-quantified as the ratio of the target protein band intensity to the intensity of the α-tubulin band. The band images were scanned using an ImageQuant 350 Analyzer (Amersham; Cytiva) and semi-quantified using the ImageQuant TL (version 8.1; Amersham; Cytiva).

Immunofluorescence microscopy. Melanocytes (~2x10^4 cells per well) were permeabilized using 4% paraformaldehyde solution at 25˚C for 1 h and then incubated in 0.2% Triton X-100 at 25˚C for 10 min. After washing with PBS, cells were blocked with 1% BSA at 25˚C for 1 h and incubated with a primary antibody against p-CREB (1:200) at 4˚C overnight for labeling and then incubated with a secondary antibody conjugated to Alexa Fluor 488 (1:500) for 3 h in the dark at room temperature. Subsequently, the nuclei were stained using DAPI mounting media (Sigma-Aldrich; Merck KGaA) for 0.5 min at room temperature and three images were collected using a Carl Zeiss fluorescence microscope (Carl Zeiss AG).

Statistical analysis. All assays were independently repeated at least three times. All statistical parameters are presented

as the mean ± standard deviation (SD). Statistical analyses were performed using one-way analysis of variance (ANOVA) followed by Tukey's post hoc test. P<0.05 was considered to indicate a statistically significant difference.

Results

Comparison of viable and damaged keratinocytes after gomisin D, J and O treatment under UVA, UVB or non-irradiation. CCK-8 and LDH assays were performed to investigate the cytoprotective effects of gomisin D, J and O on keratinocytes. HaCaT keratinocytes were treated with gomisin D, J and O under UVA, UVB or non-irradiation conditions. The keratinocytes were exposed to 10, 20, 40, 80 μM for 1 h, respectively, aim at determining the UVA or UVB irradiation according to the result of cell viability using CCK-8 assay. Compared with the control group, UVA or UVB irradiation reduced the viability of the keratinocytes. By contrast, gomisin D and J (at concentrations of 10, 20, 40 and 80 μM) dose-dependently enhanced the viability of keratinocytes. Gomisin O (at concentrations of 10, 20, 40 and 80 μM) did not change the viability of keratinocytes. The CCK-8 analysis showed that gomisin D, J and O did not significantly change keratinocyte viability at a concentration of 30 μM (Fig. 1B and C). Therefore, 30 μM gomisin D, J and O were used in follow-up experiments (Fig. S1A-C). Keratinocyte viability decreased when keratinocytes were cultured under UVA or UVB irradiation compared with the control group. However, under UVA or UVB irradiation, it was found that the viability of keratinocytes significantly increased after gomisin D and J treatment compared with the UVA or UBV-irradiated groups. Gomisin O did not alter keratinocyte viability after UVA or UVB irradiation (Fig. 1B). Keratinocyte damage was further monitored by measuring extracellular LDH release. LDH is released from the cytoplasm of keratinocytes into the culture medium as a result of keratinocyte membrane damage and lysis. An increase in LDH activity in keratinocyte culture supernatants is correlated with the rate of cytotoxicity (27). The results demonstrated that UVA and UVB irradiation markedly promoted LDH release compared with the control group. However, gomisin D significantly reduced LDH release and gomisin J markedly reduced LDH release under UVA or UVB irradiation, compared with the UVA and UVB only groups, respectively (Fig. 1C). The aforementioned experimental results showed that the antiproliferative and cytotoxic effects of UVA or UVB irradiation on keratinocytes were alleviated by gomisin D, J and O, in that order, thereby mitigating the damage caused by UVA or UVB irradiation on keratinocytes.

Comparison of intracellular ROS production after gomisin D, J and O treatment in keratinocytes with or without UVA and UVB irradiation. Oxidative stress is associated with the development and progression of UVA- or UVB-irradiated keratinocyte damage. High levels of ROS are formed in keratinocytes due to redox state imbalance (14,15). To explore the effect of gomisin D, J and O on endogenous ROS levels in UVA- or UVB-irradiated keratinocytes, fluorescence microscopy and flow cytometry were used to analyze the intracellular fluorescence intensity of the probe CM-H2DCFDA. As a result of fluorescence microscopy, images showed slight staining in the control and gomisin D-, J- and O-treated keratinocytes and marked staining in UVA- and UVB-irradiated keratinocytes. Meanwhile, keratinocytes subjected to UVA or UVB irradiation showed reduced CM-H2DCFDA staining after gomisin D and J treatment (Fig. 2A). According to the quantified results of flow cytometry, compared with the control, the intracellular ROS level of keratinocytes was markedly elevated after irradiation with UVA or UVB only compared with the control group. In gomisin D and J treatment groups, the intracellular ROS level significantly declined under UVA or UVB irradiation compared with the UVA- or UVB-irradiated groups. Intracellular ROS levels in UVA- or UVB-irradiated cells

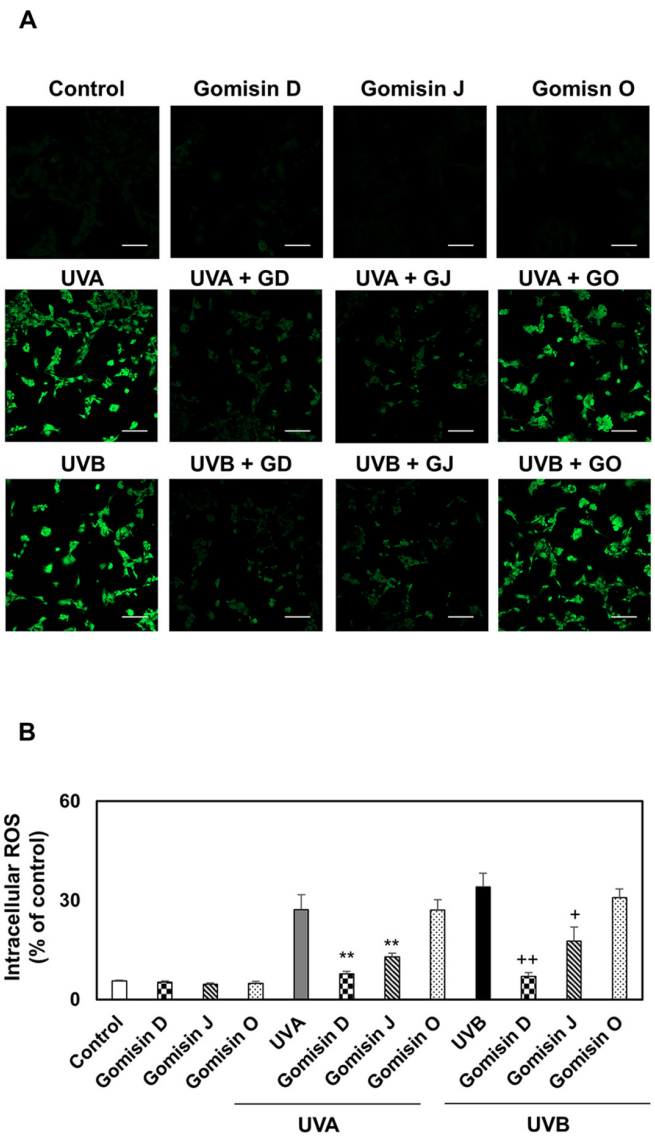

Figure 2. Intracellular ROS production of gomisin D, J and O in UVA, UVB or non-irradiated keratinocytes. HaCaT keratinocytes were pretreated with gomisin D, J and O (30 μM) for 1 h. The keratinocytes were then irradiated with UVA (20 J/cm^2) and UVB (50 mJ/cm^2) for 24 h. (A) Intracellular ROS production was visualized by Carl Zeiss fluorescence microscopy using CM-H2DCFDA staining (scale bar, 100 μm). (B) Representative flow cytometer-based quantitative analysis showed fluorescence intensity using CM-H2DCFDA staining. **P<0.01 vs. UVA-irradiated group; $^{+}$P<0.05 and $^{++}$P<0.01 vs. UVB-irradiated group. Data are expressed as the mean ± SD (n=3). UV, ultraviolet; ROS, reactive oxygen species; CM-H2DCFDA, 5-(and-6)-chloromethyl-2',7'-dichlorodihydrofluorescein diacetate acetyl ester.

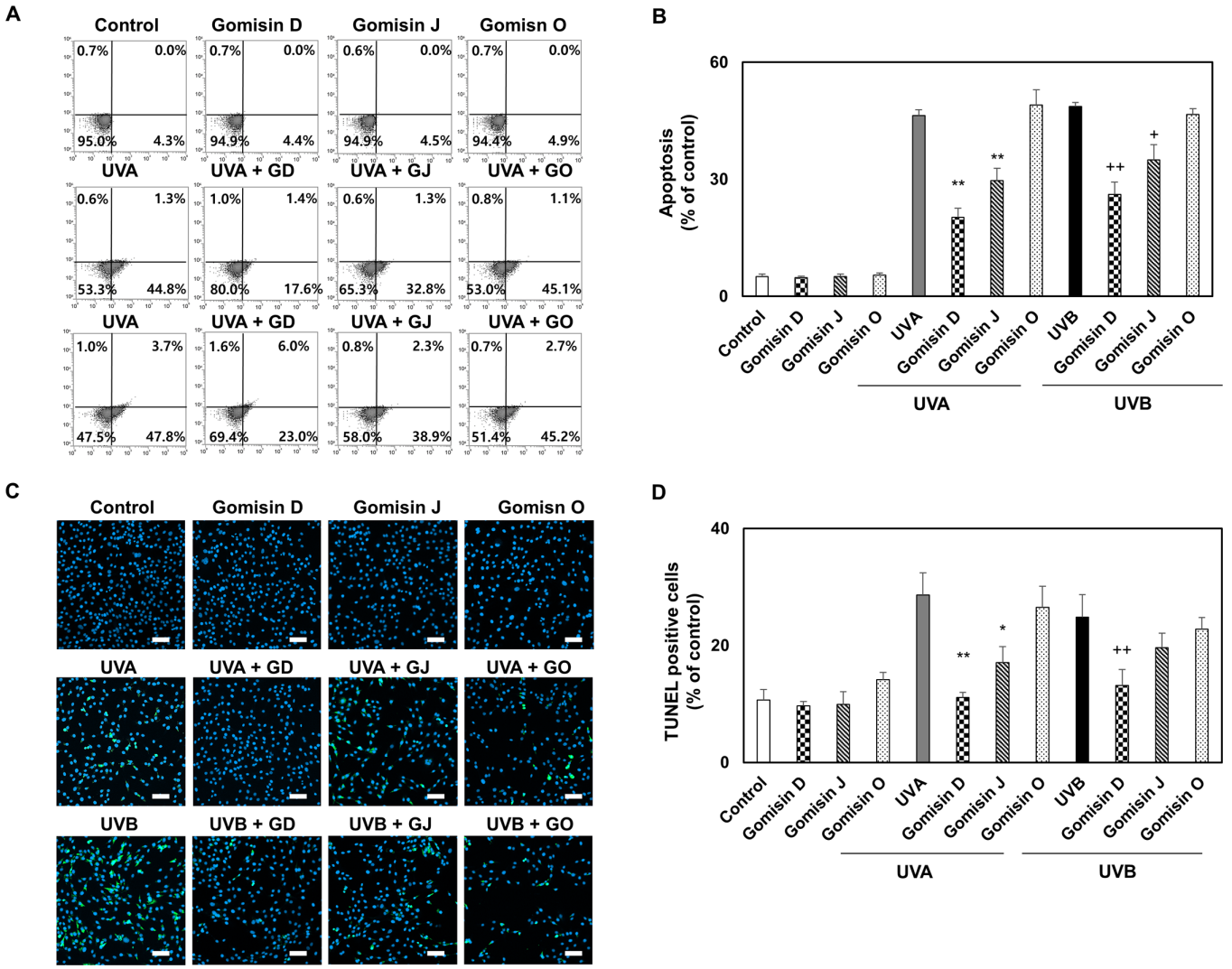

Figure 3. Apoptosis of gomisin D-, J- and O-treated keratinocytes under conditions of UVA, UVB or non-irradiation. HaCaT keratinocytes were pretreated with gomisin D, J and O (30 μM) for 1 h. The keratinocytes were then irradiated with UVA (20 J/cm^2) and UVB (50 mJ/cm^2) for 24 h. (A) Representative flow cytometer-based images and (B) quantitative analysis show fluorescence intensity using Annexin V/Dead Cell Apoptosis Kit. (C) The images of TUNEL staining for apoptosis-like cell morphology. The nuclei (blue) were labeled using DAPI (scale bar, 100 μm). (D) Percentage of TUNEL-positive cells in each treatment group. *P<0.05 and **P<0.01 vs. UVA-irradiated group; $^{+}$P<0.05 and $^{++}$P<0.01 vs. UVB-irradiated group. Data are expressed as the mean ± SD (n=3). UV, ultraviolet.

(after gomisin treatment) were inhibited at higher levels by gomisin D than gomisin J at the same concentration (Fig. 2B). These results indicated that gomisin D and J significantly inhibited UVA- or UVB-irradiated keratinocyte damage by inhibiting endogenous ROS production.

Comparison of apoptosis of keratinocytes treated with gomisin D, J and O with or without UVA and UVB irradiation. UVA and UVB irradiation of keratinocytes has been reported to lead to the inhibition of proliferation, ROS generation and apoptosis (28). To detect apoptosis, which is a reliable indicator of keratinocyte damage, keratinocytes were stained with Annexin V and PI (Annexin V/PI) and subjected to a TUNEL assay and analyzed by fluorescence microscopy and flow cytometry. Annexin V/PI flow cytometry was used to quantify apoptotic keratinocytes. The proportion of viable keratinocytes in gomisin D and J pretreatment was clearly higher than that in UVA- or UVB-irradiated keratinocytes, indicating that gomisin D and J inhibited UVA- and UVB-induced apoptosis (Fig. 3A). Quantified data from flow cytometry analysis showed that early and late apoptotic keratinocyte rates were markedly upregulated in UVA- or UVB-irradiated keratinocytes compared with the control group, whereas gomisin D and J effectively reversed these changes (Fig. 3B). UVA and UVB irradiation increased TUNEL nuclear staining activity, whereas gomisin D and J decreased the TUNEL nuclear staining activity rate under UVA and UVB irradiation. Gomisin D, J and O (30 μM) did not increase the TUNEL nuclear staining intensity compared with the control keratinocytes. As shown in Fig. 3C and D, it was confirmed that the level of apoptosis was suppressed the most by treatment with gomisin D, followed by gomisin J and then gomisin O under UVA or UVB irradiation. Overall, these results confirmed that the apoptosis of keratinocytes irradiated with UVA and UVB was inhibited by treatment with gomisin D, J and O in that order.

Comparison of intracellular melanin content and tyrosinase activity in melanocytes treated with gomisin D, J and O in

melanocytes with or without α-MSH treatment. In addition to their photoprotective properties, the effects of gomisin D, J and O on melanin synthesis in melanocytes were investigated. The viability of melanocytes was assessed via a CCK-8 assay following treatment with gomisin D, J and O (at concentration of 10, 20, 40, 80 μM). Gomisin D, J and O treatment did not alter the viability of melanocytes at 10, 20 and 40 μM for 48 h (Fig. S2A-C). On measuring the intracellular tyrosinase activity, it was found that α-MSH treatment elevated intracellular tyrosinase activity compared with the control group, whereas gomisin D suppressed intracellular tyrosinase activity in a dose-dependent manner compared with the α-MSH group. However, gomisin J and O treatment did not result in a significant difference in intracellular tyrosinase activity (Fig. S3A-C). Prior to investigating the biological potential of gomisin D, J and O in α-MSH-induced melanogenesis, the viability of B16F10 melanocytes after treatment with gomisin D, J and O (30 μM) with or without α-MSH treatment was assessed using a CCK-8 assay. Gomisin D, J and O (30 μM) did not alter cell viability compared with the controls, with or without α-MSH (Fig. 4A). Therefore, 30 μM gomisin D, J and O were used in follow-up experiments. α-MSH is a commonly known melanogenic agent that increases intracellular melanin content by activating adenylate cyclase by binding to the melanocortin 1 receptor (28). To investigate the effect of gomisin D, J and O on melanogenesis in melanocytes, the intracellular melanin content was determined by visual observation and biochemical measurements. As shown in Fig. 4B, the intracellular melanin content was significantly increased by α-MSH treatment compared with the control group, whereas co-treatment with gomisin D showed a significant reduction of the intracellular melanin content compared with that of the α-MSH treatment group (Fig. 4B). Next, the effect of gomisin D, J and O on the intracellular tyrosinase content in MSH-stimulated melanocytes was determined. As expected, the intracellular tyrosinase activity of α-MSH-stimulated melanocytes increased compared with the control group, whereas that of α-MSH-stimulated melanocytes treated with gomisin D significantly decreased compared with the α-MSH group (Fig. 4C). These results indicated that gomisin D significantly inhibited the intracellular melanin content and tyrosinase activity without altering cell viability.

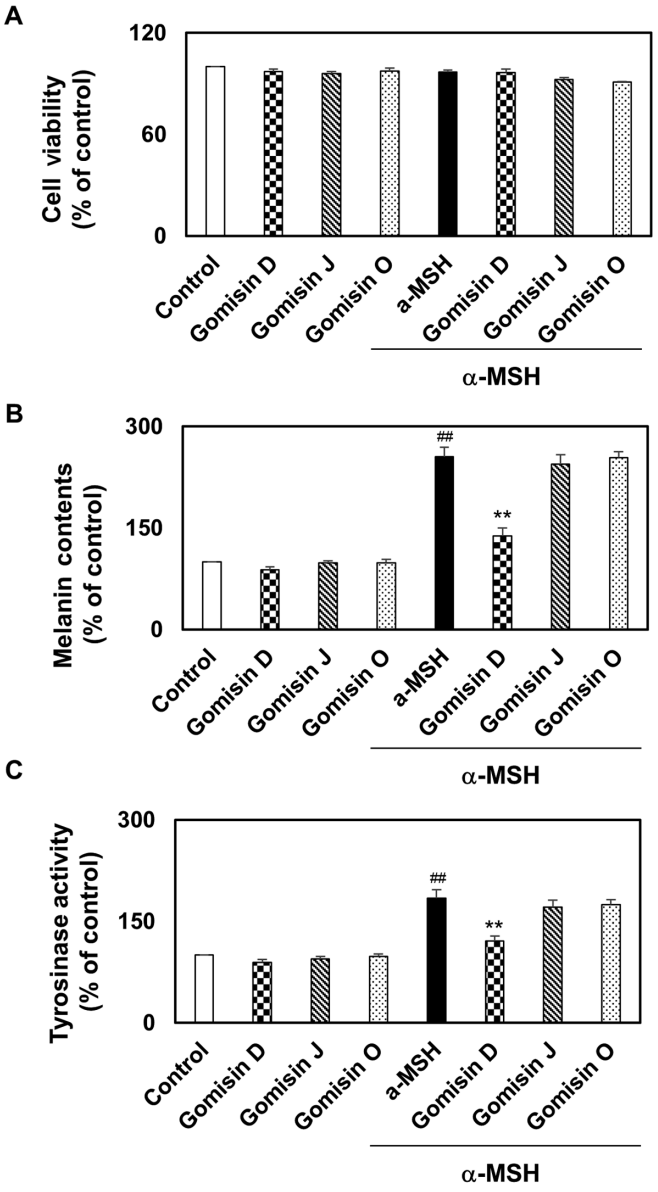

Figure 4. Melanin synthesis and tyrosinase activity in α-MSH-stimulated melanocytes. B16F10 melanocytes were pretreated with gomisin D, J and O (30 μM) for 1 h with or without α-MSH (0.5 μM). These melanocytes were maintained for 48 h. (A) The percentage of viable melanocytes was assessed via a Cell Counting Kit-8 assay. (B) Intracellular melanin content and (C) tyrosinase activity were determined. Relative mean values were calculated by normalizing the protein contents with those of the control. $^{\#\#}$P<0.01 vs. control; **P<0.01 vs. α-MSH-stimulated group. Data are expressed as the mean ± SD (n=3). UV, ultraviolet; α-MSH, α-melanocyte stimulating hormone.

Comparison of transcription and translation levels of MITF, tyrosinase, TRP-1 and TRP-2 after treatment with gomisin D, J and O in melanocytes with or without α-MSH treatment. Melanogenesis markers (tyrosinase, TRP-1 and TRP-2) are activated by MITF (23,24). Therefore, the effects of gomisin D, J and O on the protein and mRNA expression levels of MITF, tyrosinase, TRP-1 and TRP-2 were examined; the melanocytes were treated with gomisin D, J and O in the presence or absence of α-MSH. As shown in Fig. 5A-C, the mRNA levels of tyrosinase, TRP-1 and TRP-2 were significantly increased by α-MSH treatment compared with the control group. By contrast, compared with the α-MSH treatment, gomisin D significantly downregulated the mRNA levels of tyrosinase, TRP-1 and TRP-2. In addition, gomisin D, J and O alone had no significant effects on tyrosinase, TRP-1 and TRP-2 mRNA levels. Western blotting showed that α-MSH treatment increased the protein expression levels of MITF, tyrosinase, TRP-1 and TRP-2 compared with the control group, and the levels of these proteins were downregulated by co-treatment with gomisin D compared with the α-MSH group (Fig. 5D and E). These results suggested that gomisin D had the potential to promote anti-melanogenesis effects, which may play a role in the downregulation of melanogenesis markers.

Comparison of PKA and CREB phosphorylation after treatment with gomisin D, J and O in melanocytes with or without α-MSH treatment. Phosphorylation of CREB and PKA upregulates MITF expression, which can enhance

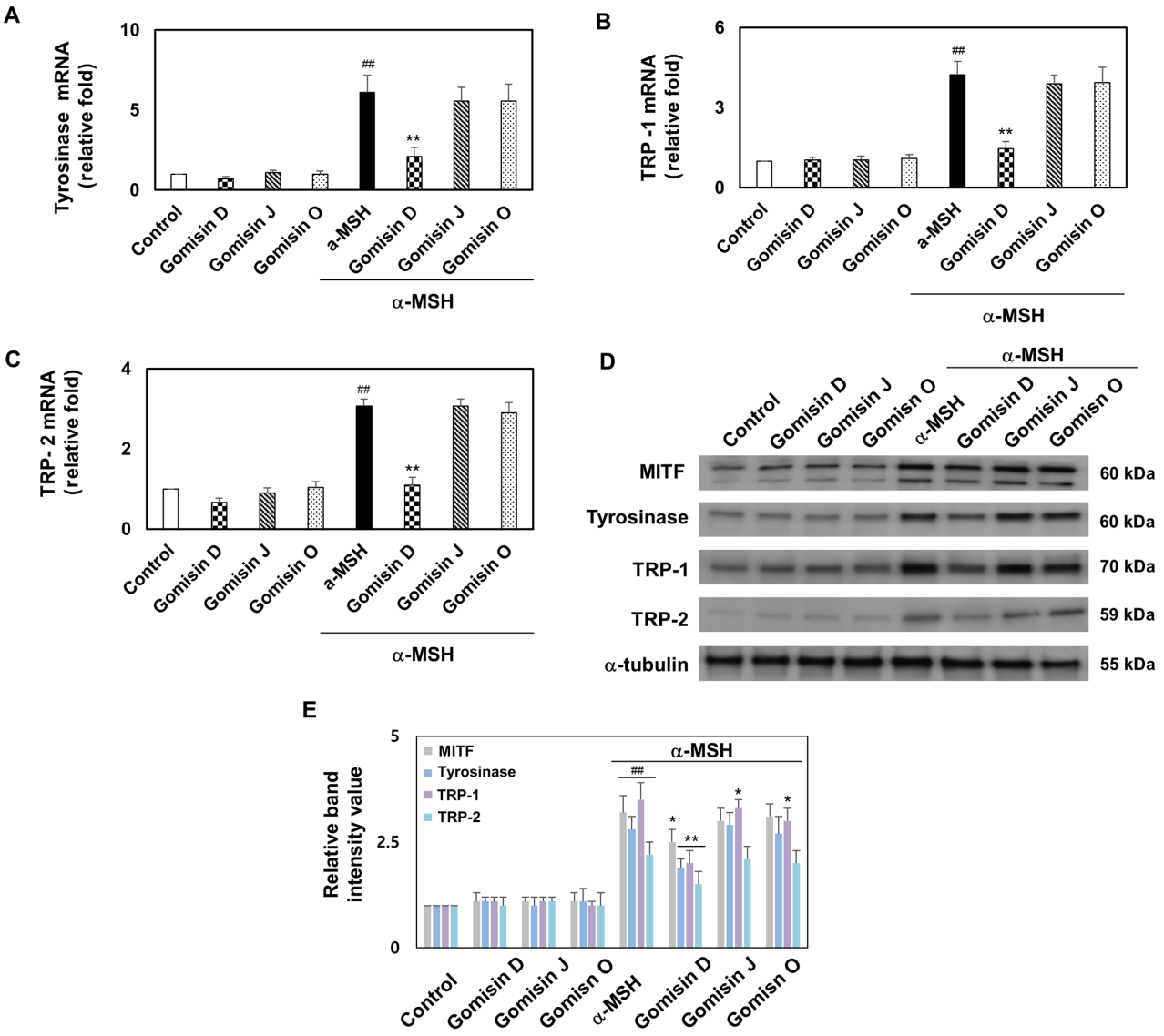

Figure 5. mRNA and protein expression of MITF, tyrosinase, TRP-1 and TRP-2 in α-MSH-stimulated melanocytes after gomisin D, J and O treatment. B16F10 melanocytes were treated with gomisin D, J and O (30 μM) for 1 h after being treated with or without α-MSH (0.5 μM). (A) Tyrosinase, (B) TRP-1 and (C) TRP-2 transcription levels were examined via reverse transcription-quantitative PCR. These melanocytes were maintained for 48 h. (D) MITF, tyrosinase, TRP-1 and TRP-2 at the translation levels were investigated by western blotting. (E) Representative statistics of MITF, tyrosinase, TRP-1 and TRP-2 protein levels of melanocytes in each group. $^{\#\#}$P<0.01 vs. control; *P<0.05 and **P<0.01 vs. α-MSH-stimulated group. Data are expressed as the mean ± SD (n=3). UV, ultraviolet; α-MSH, α-melanocyte stimulating hormone; MITF, microphthalmia-associated transcription factor; TRP-1, tyrosinase-related protein-1; TRP-2, tyrosinase-related protein-2.

melanogenesis in melanocytes (23). PKA and CREB phosphorylation was detected by western blotting to further explore the potential regulatory mechanisms underlying the effects of gomisin D, J and O on α-MSH-induced melanogenesis. Western blot analysis indicated that gomisin D effectively inhibited the increase in the phosphorylation levels of PKA and CREB caused by α-MSH treatment. In addition, gomisin D, J and O alone had negligible effects on the phosphorylation levels of PKA and CREB (Fig. 6A and B). Immunofluorescence analysis was performed to observe the phosphorylation of CREB in α-MSH-stimulated melanocytes. Immunofluorescence analysis also revealed a clear decrease in the phosphorylation levels of CREB in gomisin D compared with that in the α-MSH treatment group (Fig. 6C). These results indicated that gomisin D suppressed melanogenesis in melanocytes, at least in part, through PKA and CREB phosphorylation.

Discussion

In recent years, the use of natural products and bioactive compounds has increased worldwide (29,30). A number of studies have been conducted on the efficacy of bioactive compounds in the development of natural products (31-33). Brightening candidates from natural products are non-toxic and can be safely used in cosmetic and pharmaceutical formulations to aid in the development of efficient natural brightening agents (6). Natural products are of increasing interest due to their potential antioxidant, anti-inflammatory, antitumor and antibacterial activities (34,35). Based on the properties of photoprotection and melanogenesis, several cosmetic and pharmaceutical candidates with antioxidant, photoprotective and anti-melanogenic effects have been investigated (31,36,37). Dibenzocyclooctadiene lignans are one of the most widely used biologically active compounds extracted from *Kadsura*

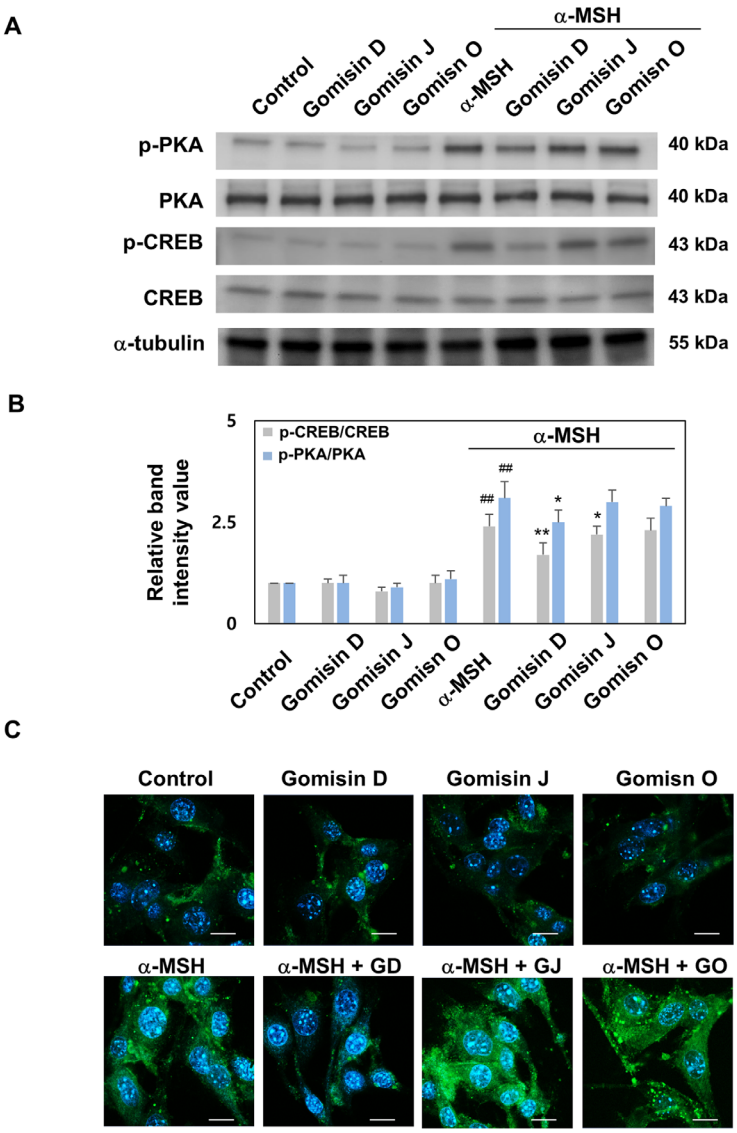

Figure 6. PKA and CREB phosphorylation levels in α-MSH-stimulated melanocytes after gomisin D, J and O treatment. B16F10 melanocytes were pre-treated with gomisin D, J and O (30 μM) for 1 h with or without α-MSH (0.5 μM). These melanocytes were maintained for 48 h. (A) PKA and CREB phosphorylation levels were studied by western blotting. (B) Representative statistics of the PKA and CREB phosphorylation levels of melanocytes in each group. (C) Co-immunofluorescence staining of p-CREB (green), the nuclei were labeled using DAPI (blue). Scale bar, 10 μm. $^{\#\#}$P<0.01 vs. control. *P<0.05 and **P<0.01 vs. α-MSH-stimulated group. Data are expressed as the mean ± SD (n=3). UV, ultraviolet; α-MSH, α-melanocyte stimulating hormone; CREB, cAMP response element binding protein; PKA, protein kinase A; p-, phosphorylated.

medicinal plants in China and other Asian countries (2,38). Studies have confirmed that *Kadsura* medicinal plants exert various pharmacological effects, including anti-HIV, anti-fungal, anti-lipid peroxidation, anti-hepatitis, anti-inflammatory and antitumor properties, and are widely used in the treatment of rheumatoid arthritis and promoting blood and fluid circulation (39-41). Dibenzocyclooctadiene lignans have been shown to possess the potential for use in several cosmetic and pharmaceutical applications. Several studies have identified the antioxidant, photoprotective and anti-melanogenic effects of natural extracts rich in dibenzocyclooctadiene lignans, such as that in *Kadsura* medicinal plants (42-44). The aforementioned evidence suggests that dibenzocyclooctadiene lignans may be useful as cosmetic and pharmaceutical candidates (45-47). However, to the best of our knowledge, the mechanisms responsible for the photoprotective and anti-melanogenic effects of gomisin D, J and O are not yet fully understood.

In the present study, UVA- and UVB-irradiated keratinocyte models were initially used to establish a more rational anti-phototoxicity strategy. Based on the important cellular events indicated by the analysis, the photoprotective properties of gomisin D, J and O were evaluated by determining cell viability, LDH release, intracellular ROS accumulation and apoptosis. The functional verification experiment demonstrated that gomisin D and J had protective effects on UVA- and UVB-irradiated keratinocytes *in vitro*, including promoting keratinocyte survival under damage and reducing LDH release. Oxidative stress induces apoptosis, and keratinocyte dysfunction is considered a potential mechanism of UVA- and UVB-induced phototoxicity (48). In the current study, UVA and UVB irradiation was found to stimulate an increase in intracellular ROS levels and induce oxidative stress. Consequently, gomisin D and J could effectively modulate ROS levels and attenuate keratinocyte damage caused by oxidative stress. However, gomisin O treatment did not result

in a significant difference in ROS levels. It was also found that the protective effects of gomisin D and J were associated with the inhibition of UVA- and UVB-irradiated apoptosis.

α-MSH stimulates G protein-coupled activation of adenylate cyclase, leading to the accumulation of intracellular cAMP levels resulting in an increased level of binding to the regulatory subunit of PKA (49). Previous studies have shown that the method of inducing melanogenesis using α-MSH has been widely accepted and applied (50,51). Therefore, the present study was performed based on the construction of a model of melanocytes stimulated with α-MSH. It was found that gomisin D inhibited α-MSH-stimulated intracellular melanin content and tyrosinase activity. In addition, gomisin D downregulated the transcription and translation of melanogenic markers, such as tyrosinase, TRP-1 and TRP-2, in melanocytes stimulated with α-MSH. Tyrosinase, TRP-1 and TRP-2 are essential processes in melanogenesis regulated by MITF expression. PKA and CREB have attracted increasing research interest and are considered to be potential therapeutic targets for melanogenesis (24,49,50). Thus, the effects of PKA/CREB-modulating compounds observed during *in vivo* and *in vitro* studies are likely to be a combination of other factors. MITF is a key factor in the transcription of melanogenesis-related enzymes and the central regulator of melanogenesis (51). α-MSH leads to the expression of MITF through a signaling mechanism involving CREB, which then enters the nucleus with the M-box sequence (AGTCATGTGCT) to promote the transcription of specific melanogenic genes and enzymes (25). It is also known that PKA/CREB is stimulated by α-MSH, which binds to the CRE consensus element in the MITF promoter to upregulate MITF transcription (51). Therefore, the present study investigated MITF protein expression and PKA/CREB phosphorylation in α-MSH-stimulated melanocytes. Similarly, in this study, it was found that gomisin D suppressed α-MSH-mediated MITF protein expression and PKA/CREB phosphorylation in melanocytes. However, the results of this study are limited to cells (normal human keratinocytes and normal human melanocytes), while animal experiments were not performed, thus the exact dosing, skin layer penetration and side effects unknown in the pharmaceutical field of gomisin D in cosmetics were not investigated. Further experiments showing that gomisin D inhibits photoprotection and melanogenesis are still required. In conclusion, the potential photoprotective and anti-melanogenic properties of dibenzocyclooctadiene lignans (gomisin D, J and O) were established in this study. Gomisin D may have photoprotective and anti-melanogenic effects on keratinocytes and melanocytes. This article provides a rationale and research strategy for cosmetic and pharmaceutical interventions for the preparation of brightening and photoprotective natural compounds.

Acknowledgements

Not applicable.

Funding

This work was supported by the National Research Foundation of Korea (NRF) grant funded by the Korean government (MSIT) (grant nos. NRF-2021R1I1A3044431 and NRF-2021R1I1A3A04035369).

Availability of data and materials

The datasets used and/or analyzed during the current study are available from the corresponding author on reasonable request.

Authors' contributions

JSJ, SYP and YWC designed the study, analyzed the data and wrote the manuscript. JSJ and HMK performed the experiments. SYP and YWC confirm the authenticity of the raw data. All authors have read and approved the final manuscript.

Ethics approval and consent to participate

Not applicable.

Patient consent for publication

Not applicable.

Competing interests

The authors declare that they have no competing interests.

References

1. Woo MH, Nguyen DH, Choi JS, Park SE, Thuong PT, Min BS and Le DD: Chemical constituents from the roots of *Kadsura coccinea* with their protein tyrosine phosphatase 1B and acetylcholinesterase inhibitory activities. Arch Pharm Res 43: 204-213, 2020.
2. Huang SZ, Duan LP, Wang H, Mei WL and Dai HF: Two new AChE inhibitors isolated from Li folk herb Heilaohu '*Kadsura coccinea*' stems. Molecules 24: 3628, 2019.
3. Park SY, Bae YS, Ko MJ, Lee SJ and Choi YW: Comparison of anti-inflammatory potential of four different dibenzocyclooctadiene lignans in microglia; action via activation of PKA and Nrf-2 signaling and inhibition of MAPK/STAT/NF-κB pathways. Mol Nutr Food Res 58: 738-748, 2014.
4. Kang K, Lee KM, Yoo JH, Lee HJ, Kim CY and Nho CW: Dibenzocyclooctadiene lignans, gomisins J and N inhibit the Wnt/β-catenin signaling pathway in HCT116 cells. Biochem Biophys Res Commun 428: 285-291, 2012.
5. Svobodová A and Vostálová J: Solar radiation induced skin damage: Review of protective and preventive options. Int J Radiat Biol 86: 999-1030, 2010.
6. Wang PW, Hung YC, Lin TY, Fang JY, Yang PM, Chen MH and Pan TL: Comparison of the biological impact of UVA and UVB upon the skin with functional proteomics and immunohistochemistry. Antioxidants 8: 569, 2019.
7. Hseu YC, Chen XZ, Vudhya Gowrisankar Y, Yen HR, Chuang JY and Yang HL: The skin-whitening effects of ectoine via the suppression of α-MSH-stimulated melanogenesis and the activation of antioxidant Nrf2 pathways in UVA-irradiated keratinocytes. Antioxidants 9: 63, 2020.
8. Slominski AT, Zmijewski MA, Skobowiat C, Zbytek B, Slominski RM and Steketee JD: Sensing the environment: Regulation of local and global homeostasis by the skin's neuroendocrine system. Adv Anat Embryol Cell Biol 212: v, vii, 1-115, 2012.
9. Slominski AT, Zmijewski MA, Plonka PM, Szaflarski JP and Paus R: How UV light touches the brain and endocrine system through skin, and why. Endocrinology 159: 1992-2007, 2018.
10. Deng H, Li H, Ho ZY, Dai XY, Chen Q, Li R, Liang B and Zhu H: Pterostilbene's protective effects against photodamage caused by UVA/UVB irradiation. Pharmazie 73: 651-658, 2018.
11. Gęgotek A, Ambrożewicz E, Jastrząb A, Jarocka-Karpowicz I and Skrzydlewska E: Rutin and ascorbic acid cooperation in antioxidant and antiapoptotic effect on human skin keratinocytes and fibroblasts exposed to UVA and UVB radiation. Arch Dermatol Res 311: 203-219, 2019.

12. Gęgotek A, Jastrząb A, Jarocka-Karpowicz I, Muszyńska M and Skrzydlewska E: The effect of sea buckthorn (*Hippophae rhamnoides* L.) seed oil on UV-induced changes in lipid metabolism of human skin cells. Antioxidants 7: 110, 2018.
13. Działo M, Mierziak J, Korzun U, Preisner M, Szopa J and Kulma A: The potential of plant phenolics in prevention and therapy of skin disorders. Int J Mol Sci 17: 160, 2016.
14. Marabini L, Melzi G, Lolli F, Dell'Agli M, Piazza S, Sangiovanni E and Marinovich M: Effects of *Vitis vinifera* L. leaves extract on UV radiation damage in human keratinocytes (HaCaT). J Photochem Photobiol B 204: 111810, 2020.
15. Muzaffer U, Paul VI, Prasad NR, Karthikeyan R and Agilan B: Protective effect of *Juglans regia* L. against ultraviolet B radiation induced inflammatory responses in human epidermal keratinocytes. Phytomedicine 42: 100-111, 2018.
16. Maciel B, Moreira P, Carmo H, Gonçalo M, Lobo JMS and Almeida IF: Implementation of an *in vitro* methodology for phototoxicity evaluation in a human keratinocyte cell line. Toxicol In Vitro 61: 104618, 2019.
17. Orlow SJ, Zhou BK, Chakraborty AK, Drucker M, Pifko-Hirst S and Pawelek JM: High-molecular-weight forms of tyrosinase and the tyrosinase-related proteins: Evidence for a melanogenic complex. J Invest Dermatol 103: 196-201, 1994.
18. Slominski A, Zmijewski MA and Pawelek J: L-tyrosine and L-dihydroxyphenylalanine as hormone-like regulators of melanocyte functions. Pigment Cell Melanoma Res 25: 14-27, 2012.
19. Slominski A, Tobin DJ, Shibahara S and Wortsman J: Melanin pigmentation in mammalian skin and its hormonal regulation. Physiol Rev 84: 1155-1228, 2004.
20. Pawelek JM: Approaches to increasing skin melanin with MSH analogs and synthetic melanins. Pigment Cell Res 14: 155-160, 2001.
21. Kim BH, Hong SN, Ye SK and Park JY: Evaluation and optimization of the anti-melanogenic activity of 1-(2-cyclohexylmethoxy-6-hydroxy-phenyl)-3-(4-hydroxymethyl-phenyl)-propenone derivatives. Molecules 24: 1372, 2019.
22. Jung HJ, Lee AK, Park YJ, Lee S, Kang D, Jung YS, Chung HY and Moon HR: (2E,5E)-2,5-bis(3-hydroxy-4-methoxybenzylidene) cyclopentanone exerts anti-melanogenesis and anti-wrinkle activities in B16F10 melanoma and Hs27 fibroblast cells. Molecules 23: 1415, 2018.
23. Azam MS, Kwon M, Choi J and Kim HR: Sargaquinoic acid ameliorates hyperpigmentation through cAMP and ERK-mediated downregulation of MITF in α-MSH-stimulated B16F10 cells. Biomed Pharmacother 104: 582-589, 2018.
24. Seo GY, Ha Y, Park AH, Kwon OW and Kim YJ: *Leathesia difformis* extract inhibits α-MSH-induced melanogenesis in B16F10 cells via down-regulation of CREB signaling pathway. Int J Mol Sci 20: 536, 2019.
25. Park SY, Jin ML, Kim YH, Kim Y and Lee SJ: Aromatic-turmerone inhibits α-MSH and IBMX-induced melanogenesis by inactivating CREB and MITF signaling pathways. Arch Dermatol Res 303: 737-744, 2011.
26. Livak KJ and Schmittgen TD: Analysis of relative gene expression data using real-time quantitative PCR and the 2(-Delta Delta C(T)) Method. Methods 25: 402-408, 2001.
27. Lee J, Kim HJ, Lee SJ and Lee MS: Effects of *Hahella chejuensis*-derived prodigiosin on UV-induced ROS production, inflammation and cytotoxicity in HaCaT human skin keratinocytes. J Microbiol Biotechnol 31: 475-482, 2021.
28. Kim JH, Lee JE, Kim T, Yeom MH, Park JS, di Luccio E, Chen H, Dong Z, Lee KW and Kang NJ: 7,3',4'-trihydroxyisoflavone, a metabolite of the soy isoflavone daidzein, suppresses α-melanocyte-stimulating hormone-induced melanogenesis by targeting melanocortin 1 receptor. Front Mol Biosci 7: 577284, 2020.
29. Li W, Yuan G, Pan Y, Wang C and Chen H: Network pharmacology studies on the bioactive compounds and action mechanisms of natural products for the treatment of diabetes mellitus: A review. Front Pharmacol 8: 74, 2017.
30. Anand M and Basavaraju R: A review on phytochemistry and pharmacological uses of *Tecoma stans* (L.) Juss. ex Kunth. J Ethnopharmacol 265: 113270, 2021.
31. Piazza S, Fumagalli M, Khalilpour S, Martinelli G, Magnavacca A, Dell'Agli M and Sangiovanni E: A review of the potential benefits of plants producing berries in skin disorders. Antioxidants 9: 542, 2020.
32. Pundir S, Garg P, Dviwedi A, Ali A, Kapoor VK, Kapoor D, Kulshrestha S, Lal UR and Negi P: Ethnomedicinal uses, phytochemistry and dermatological effects of *Hippophae rhamnoides* L.: A review. J Ethnopharmacol 266: 113434, 2021.
33. Sitarek P, Kowalczyk T, Wieczfinska J, Merecz-Sadowska A, Górski K, Śliwiński T and Skała E: Plant extracts as a natural source of bioactive compounds and potential remedy for the treatment of certain skin diseases. Curr Pharm Des 26: 2859-2875, 2020.
34. Zaid AN and Al Ramahi R: Depigmentation and anti-aging treatment by natural molecules. Curr Pharm Des 25: 2292-2312, 2019.
35. Desmedt B, Courselle P, De Beer JO, Rogiers V, Grosber M, Deconinck E and De Paepe K: Overview of skin whitening agents with an insight into the illegal cosmetic market in Europe. J Eur Acad Dermatol Venereol 30: 943-950, 2016.
36. Kemboi D, Peter X, Langat M and Tembu J: A review of the ethnomedicinal uses, biological activities, and triterpenoids of *Euphorbia* species. Molecules 25: 4019, 2020.
37. Wang L, Jayawardena TU, Yang HW, Lee HG and Jeon YJ: The potential of sulfated polysaccharides isolated from the brown seaweed ecklonia maxima in cosmetics: Antioxidant, anti-melanogenesis, and photoprotective activities. Antioxidants 9: 724, 2020.
38. Liu J, Qi Y, Lai H, Zhang J, Jia X, Liu H, Zhang B and Xiao P: Genus *Kadsura*, a good source with considerable characteristic chemical constituents and potential bioactivities. Phytomedicine 21: 1092-1097, 2014.
39. Yang Y, Liu Y, Daniyal M, Yu H, Xie Q, Li B, Jian Y, Man R, Wang S, Zhou X, *et al*: New Lignans from roots of *Kadsura coccinea*. Fitoterapia 139: 104368, 2019.
40. Liu J, Wei X, Zhang X, Qi Y, Zhang B, Liu H and Xiao P: A comprehensive comparative study for the authentication of the *Kadsura* crude drug. Front Pharmacol 9: 1576, 2019.
41. Sritalahareuthai V, Aursalung A, On-Nom N, Temviriyanukul P, Charoenkiatkul S and Suttisansanee U: Nutritional composition of conserved *Kadsura* spp. plants in Northern Thailand. Heliyon 6: e04451, 2020.
42. Chiu PY, Lam PY, Yan CW and Ko KM: Schisandrin B protects against solar irradiation-induced oxidative injury in BJ human fibroblasts. Fitoterapia 82: 682-691, 2011.
43. Gao C, Chen H, Niu C, Hu J and Cao B: Protective effect of Schizandrin B against damage of UVB irradiated skin cells depend on inhibition of inflammatory pathways. Bioengineered 8: 36-44, 2017.
44. Lee J, Ryu HS, Kim JM, Jung TH, Park SM and Lee YM: Anti-melanogenic effect of gomisin N from *Schisandra chinensis* (Turcz.) Baillon (Schisandraceae) in melanoma cells. Arch Pharm Res 40: 807-817, 2017.
45. Zheng X, Feng F, Jiang X, Qiu J, Cai X and Xiang Z: A rapid UPLC-MS method for quantification of gomisin D in rat plasma and its application to a pharmacokinetic and bioavailability study. Molecules 24: 1403, 2019.
46. Zhang AH, Yu JB, Sun H, Kong L, Wang XQ, Zhang QY and Wang XJ: Identifying quality-markers from Shengmai San protects against transgenic mouse model of Alzheimer's disease using chinmedomics approach. Phytomedicine 45: 84-92, 2018.
47. Szopa A, Dziurka M, Warzecha A, Kubica P, Klimek-Szczykutowicz M and Ekiert H: Targeted lignan profiling and anti-inflammatory properties of *Schisandra rubriflora* and *Schisandra chinensis* extracts. Molecules 23: 3103, 2018.
48. Dubey D, Chopra D, Singh J, Srivastav AK, Kumari S, Verma A and Ray RS: Photosensitized methyl paraben induces apoptosis via caspase dependent pathway under ambient UVB exposure in human skin cells. Food Chem Toxicol 108: 171-185, 2017.
49. Park JU, Yang SY, Guo RH, Li HX, Kim YH and Kim YR: Anti-melanogenic effect of *Dendropanax morbiferus* and its active components via protein kinase A/cyclic adenosine monophosphate-responsive binding protein- and p38 mitogen-activated protein kinase-mediated microphthalmia-associated transcription factor downregulation. Front Pharmacol 11: 507, 2020.
50. Hwang YS, Oh SW, Park SH, Lee J, Yoo JA, Kwon K, Park SJ, Kim J, Yu E, Cho JY, *et al*: Melanogenic effects of maclurin are mediated through the activation of cAMP/PKA/CREB and p38 MAPK/CREB signaling pathways. Oxid Med Cell Longev 2019: 9827519, 2019.
51. Kang B, Kim Y, Park TJ and Kang HY: Dasatinib, a second-generation tyrosine kinase inhibitor, induces melanogenesis via ERK-CREB-MITF-tyrosinase signaling in normal human melanocytes. Biochem Biophys Res Commun 523: 1034-1039, 2020.